Bioorganic & Medicinal Chemistry Letters 21 (2011) 1243–1247

Contents lists available at ScienceDirect

Bioorganic & Medicinal Chemistry Letters

journal homepage: www.elsevier.com/locate/bmcl

Non-oxime inhibitors of B-Raf^{V600E} kinase

Li Ren [a], Steve Wenglowsky [a,*], Greg Miknis [a], Bryson Rast [a], Alex J. Buckmelter [a], Robert J. Ely [a], Stephen Schlachter [a], Ellen R. Laird [a], Nikole Randolph [a], Michele Callejo [a], Matthew Martinson [a], Sarah Galbraith [a], Barbara J. Brandhuber [a], Guy Vigers [a], Tony Morales [a], Walter C. Voegtli [a], Joseph Lyssikatos [b]

[a] Array BioPharma, 3200 Walnut Street, Boulder, CO 80301, United States
[b] Genentech, Inc., 1 DNA Way, South San Francisco, CA 94080-4990, United States

ARTICLE INFO

Article history:
Received 15 October 2010
Revised 10 December 2010
Accepted 15 December 2010
Available online 19 December 2010

Keywords:
B-Raf
Furopyridine
Indazole

ABSTRACT

The development of inhibitors of B-Raf^{V600E} serine–threonine kinase is described. Various head-groups were examined to optimize inhibitor activity and ADME properties. Several of the head-groups explored, including naphthol, phenol and hydroxyamidine, possessed good activity but had poor pharmacokinetic exposure in mice. Exposure was improved by incorporating more metabolically stable groups such as indazole and tricyclic pyrazole, while indazole could also be optimized for good cellular activity.

The Ras/Raf/MEK/ERK (MAPK) signaling pathway transduces signals from cell surface receptors to the nucleus leading to cellular proliferation, differentiation and survival.[1] Mutations in the *BRAF* gene may lead to MAPK pathway amplification via constitutive activation of B-Raf kinase and are present in ~7% of all cancers.[2] Mutated B-Raf is most frequently associated with melanoma and has been detected in up to 82% of cutaneous melanocyte nevi,[3] 66% of primary melanomas[2] and 40–68% of metastatic melanomas.[4] Over 90% of detected mutations in B-Raf are a single glutamic acid for valine substitution at residue 600 (V600E)[2] which leads to constitutive kinase activity 500-fold greater than B-Raf^{WT} and correlates with increased malignancy and decreased response to chemotherapy.[5,6] Thus, small-molecule inhibition of B-Raf^{V600E} is a promising strategy in oncology drug development.[7]

In the previous paper we described a series of furopyridine inhibitors of B-Raf^{V600E} (Fig. 1).[8] While several of these inhibitors demonstrated good enzymatic and cellular inhibition of B-Raf, they displayed insufficient plasma exposure in rodents for in vivo efficacy. The poor pharmacokinetics of this series was attributed to oxime metabolism.[8,9] In an effort to improve inhibitor pharmacokinetics while maintaining activity against B-Raf, several replacements of the indanone–oxime head-group were explored.

X-ray crystallography revealed several critical interactions between furopyridines and the ATP cleft of the B-Raf catalytic domain (Fig. 2). The template forms several hydrophobic interactions with residues of the P-loop, the hinge, and the floor of the ATP pocket. The pyridine of the bicyclic core makes a hydrogen bond at the hinge region of the active site to the –NH of Cys532. The indanone moiety occupies the hydrophobic pocket adjacent to the gatekeeper residue Thr529, while the oxime makes two key interactions: the sp^2 nitrogen acts as an acceptor from the sidechain amine of the catalytic lysine (Lys483) and the hydroxyl group acts as a donor to Glu501 of the C-helix. Initially, we sought to develop a head-group which would make the same interactions with the enzyme as the oxime.

Structure–activity relationships were developed for each head-group by varying the substitution at the 2-position of the furopyridine. Initially, inhibitors were designed that would make one or both of the interactions achieved by the oxime; the activities of these compounds are provided in Table 1. Indanones **2a** and **2b** were significantly less active against B-Raf in both the

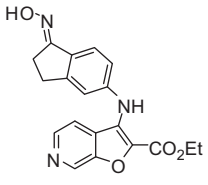

B-Raf IC_{50} = <2 nM
pERK IC_{50} = 30 nM

Figure 1. Furopyridine inhibitor **1**.

* Corresponding author. Tel.: +1 303 386 1123.
E-mail address: swenglowsky@arraybiopharma.com (S. Wenglowsky).

0960-894X/$ - see front matter © 2010 Elsevier Ltd. All rights reserved.
doi:10.1016/j.bmcl.2010.12.061

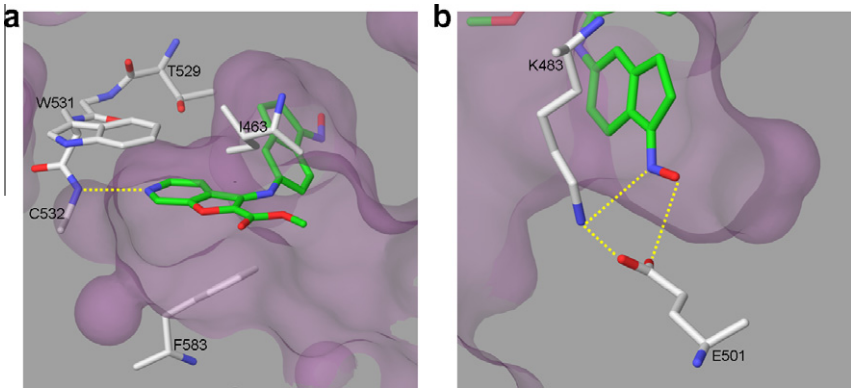

Figure 2. X-ray crystal structure of furopyridine inhibitor **1** (3.7 Å resolution). Hydrogen bonding interactions are illustrated by dashed yellow lines. (a) View of the hinge-binding template. For clarity, sidechains are depicted only for those residues that make specific hydrophobic contacts. (b) Close-up of electronic interactions involving the oxime.

Table 1
B-Raf^{V600E} activity of indanones, hydroxyamidines and pyrazoles

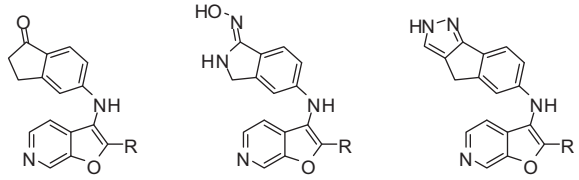

2 **3** **4**

Compound	R	B-Raf IC_{50}[a] (nM)	pERK IC_{50}[a] (nM)
2a		93.0	6800
2b		16.0	820
3a		5.2	1300
3b		0.5	18
4a		38.0	7800
4b	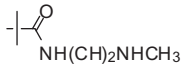	42.9	4600
4c		4.0	1100

[a] Values are means of three experiments.

biochemical (B-Raf^{V600E}) and cellular assays,[10] most likely due to the loss of the hydrogen bond with Glu501. Hydroxyamidines **3a** and **3b** possess the same hydrogen bonding interactions as oximes.[11] Isopropyl amide **3a**, while showing excellent activity in the biochemical assay, was poorly active in the cellular assay. Substituting the amide in **3a** for 2-pyrimidine provided compound **3b** and a 70-fold increase in cellular activity. Unfortunately, this compound suffered from rapid clearance in vivo.[8,12] In an attempt to improve these poor properties while maintaining the interactions of the oxime and hydroxyamidine, the tricyclic pyrazole compounds **4a–c** were prepared. However, none of the analogs provided the necessary level of cellular activity and other head-group replacements were pursued.

Table 2
B-Raf^{V600E} activity of naphthyl analogs **5–9**

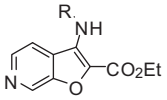

Compound	R	B-Raf IC_{50}[a] (nM)	pERK IC_{50}[a] (nM)
5	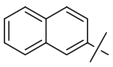	179	–
6	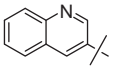	30.0	5000
7	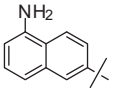	52.0	9100
8	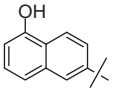	1.1	54
9	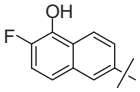	3.0	142

[a] Values are means of three experiments.

Naphthyl head-groups were prepared and their biochemical and cellular activities are provided in Table 2. Initial SAR studies conserved the ethyl ester at the 2-position of the furopyridine core while substitutions on the naphthyl group were examined. Unsubstituted naphthyl **5** was weakly active in the biochemical assay. Quinoline **6** and 1-aminonaphthyl **7** were only moderately more active than the naphthyl analog. An appropriately positioned hydroxyl group on the naphthyl head-group (**8**) provided the naphthol inhibitor class that was of comparable potency to the oximes. Fluorination at the 2-position adjacent to the hydroxyl group (**9**) led to a small loss of biochemical and cellular activity, likely due to reduced acceptor ability of the hydroxyl. The excellent potency of the naphthol series can be explained by the dual donor/acceptor capability of the hydroxyl group; this group binds to Lys483 and Glu501 similarly to oximes with only a minor movement of the Glu501 sidechain (Fig. 3a).[13]

The naphthol series was substituted with both amides and 2-pyrimidines at the 2-position on the furopyridine core (Table 3). Replacement of the ethyl ester of compound **8** with various amides gave potent compounds bearing both lipophilic

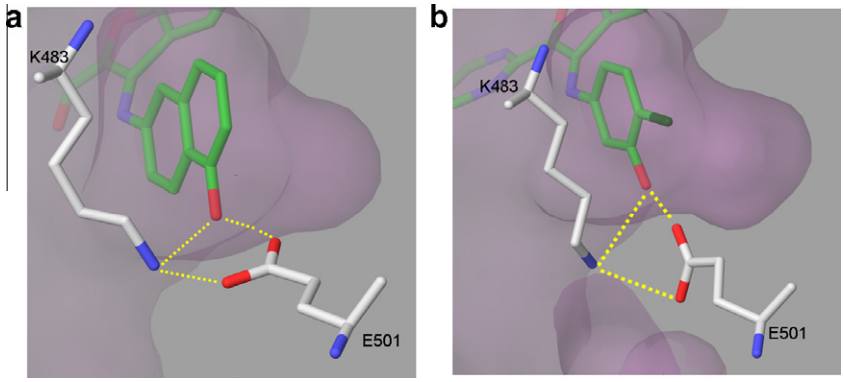

Figure 3. X-ray crystal structures of B-Raf in complex with naphthols and phenols. The orientation is comparable to that shown in Figure 2b. (a) Naphthol **12** forms hydrogen bonds to Lys483 and Glu501. Relative to the oxime depicted in Figure 2b, the sidechain of Glu501 is rotated ca. 20 degrees about chi1 (3.0 Å resolution). (b) Chlorophenol **19** uses the chlorine to replace some of the naphthol bulk, while the 3-hydroxy group remains positioned for dual hydrogen-bond donor/acceptor ability via small movements of Lys483 and Glu501 (2.9 Å resolution).

Table 3
B-Raf^{V600E} activity of naphthol analogs **10**–**14**

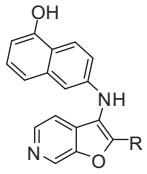

Compound	R	B-Raf IC_{50}[a] (nM)	pERK IC_{50}[a] (nM)
10		1.4	86.7
11	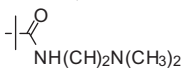	5.0	102
12	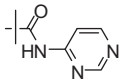	1.4	37.9
13		1.0	4.1
14	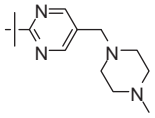	2.0	16

[a] Values are means of three experiments.

Table 4
B-Raf^{V600E} activity of chlorophenol analogs **15**–**19**

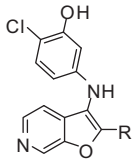

Compound	R	B-Raf IC_{50}[a] (nM)	pERK IC_{50}[a] (nM)
15		2.3	442
16		4.0	823
17	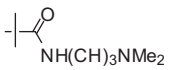	5.0	1870
18	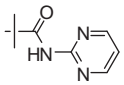	1.6	556
19		1.4	31

[a] Values are means of three experiments.

groups (**10** and **12**) and a solubilizing group (**11**). The high cellular activity of 2-pyrimidine as a furopyridine substituent was observed in the naphthol series. Compound **13** was a very potent B-Raf inhibitor and attachment of a solubilizing amine to the pyrimidine maintained significant cellular activity. Unfortunately, the pharmacokinetics across this series was consistently poor due to high clearance, likely resulting from glucuronidation of the naphthol.[14]

Chlorophenols[15] were explored concurrently to the naphthols and also displayed good activity against B-Raf (Table 4). While the ester and amide analogs (**15–18**) had excellent biochemical activity and moderate activity in the cellular assay, 2-pyrimidine substitution (**19**) gave the anticipated improvement into the desired potency range for potential in vivo efficacy. Likewise to the naphthols, the good potency of the chlorophenols can be explained by the dual donor/acceptor capability of its hydroxyl group to Lys483 and Glu501 (Fig. 3b).[13] Similarly to the naphthols however, these compounds also suffered from poor pharmacokinetic exposure.

Molecular modeling suggested that the binding interactions for an indazole head-group should be similar to those for phenol, by which the N1 hydrogen donor overlaps with the hydroxyl group.[16] Table 5 summarizes the data for several indazole-containing analogs. Compounds **20–23** demonstrate that a chloro substitution at the appropriate position (R^1) produces a significant improvement in cellular activity; this lipophilic contact is expected to project into the hydrophobic pocket adjacent to the gatekeeper residue Thr529, similarly to the chlorophenol series. Isopropyl amide **24** lost significant cellular activity compared to 2-pyrimidine, and methyl- (**25**) and fluoro- (**26**) substituted indazoles were less active than their chloro counterpart. Bis substitution on the indazole ring at R^1 and R^2 (**27**) did not demonstrate any additive improvements in cellular activity over chloroindazole **21**. However, bis substitution at R^1 and R^4 provided a slight improvement in activity in the cellular assay (**28**). Solubilizing groups were then tethered at the R^4 position of the indazole. While aminopropyl **29**

Table 5
B-Raf^{V600E} activity of indazole analogs **20–30**

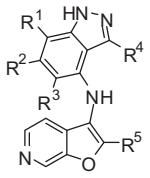

Compound	R^1	R^2	R^3	R^4	R^5	B-Raf IC_{50}[a] (nM)	pERK IC_{50}[a] (nM)
20	H	H	H	H	2-Pyrimidyl	14	2500
21	Cl	H	H	H	2-Pyrimidyl	4.2	250
22	H	Cl	H	H	2-Pyrimidyl	5.7	1600
23	H	H	Cl	H	2-Pyrimidyl	240	—
24	Cl	H	H	H	$CONHCH(CH_3)_2$	2.7	4200
25	Me	H	H	H	2-Pyrimidyl	2.4	840
26	F	H	H	H	2-Pyrimidyl	2.0	3500
27	Cl	Me	H	H	2-Pyrimidyl	0.3	300
28	Cl	H	H	Et	2-Pyrimidyl	0.8	140
29	Cl	H	H	$(CH_2)_3NH_2$	2-Pyrimidyl	4.3	1300
30	Cl	H	H	$(CH_2)_3OH$	2-Pyrimidyl	0.8	350

[a] Values are means of three experiments.

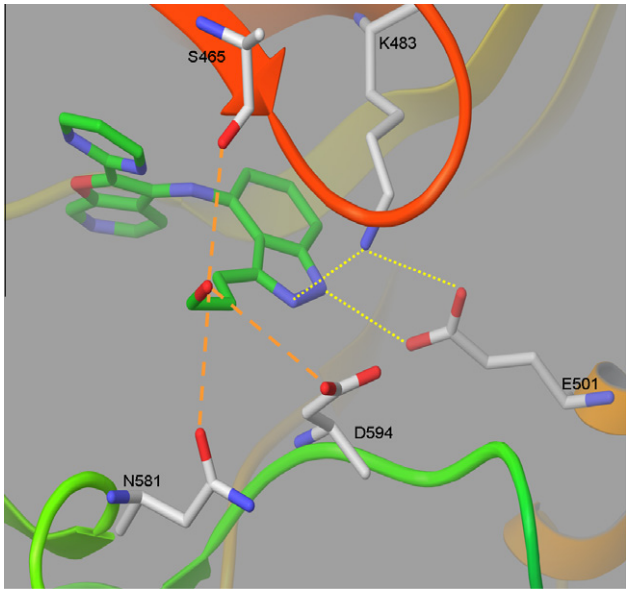

Figure 4. X-ray crystal structure of B-Raf in complex with hydroxypropyl-substituted indazole **31** (3.5 Å resolution). Hydrogen bonding interactions are depicted with yellow dotted lines. Orange dashes indicate hydrogen bonding groups that are roughly equidistant from the hydroxyl group.

was not tolerated, hydroxypropyl compound **30** could be incorporated at this position with comparable activity to compound **21**. An X-ray crystal structure of compound **31** (the analog of **30** where R^1 = H) confirmed the expected interactions for the indazole series to Lys483 and Glu501 (Fig. 4).[13] The hydroxypropyl group resides in the location usually occupied by the second phosphate group of ATP analogs, and, due to the low electron density of the group, is expected to shift position among several hydrogen bonding partners. Selectivity was obtained against a panel of 243 kinases for representative indazole **21** at 1 μM. Moderate selectivity was observed with 42 kinases demonstrating >50% inhibition, including VEGFR2. This represents an attenuation of selectivity as compared to the oxime series.[8]

While oximes, naphthols and phenols all demonstrated negligible oral absorption and/or rapid clearance in rodents, alternative head-groups such as tricyclic pyrazoles and indazoles demonstrated

Table 6
In vitro ADME and oral pharmacokinetic parameters in mice at 25 mg/kg dose for selected furopyridine

Compound	Caco-2[a]	Pred. Cl[b]	C_{max} (μg/mL)	AUC_{0-inf} (μg hr/mL)
4c	High	42	2.22	10.4
21	Low	56	c	c
23	High	9.9	3.73	17.0

[a] Caco-2 permeability classification: low (<2 × 10^{-6} cm/s), medium (2–8 × 10^{-6} cm/s), high (>8 × 10^{-6} cm/s).
[b] Mouse liver microsomes (ml/min/kg).
[c] No plasma levels were detected at any time point.

improved exposure upon oral dosing at 25 mg/kg. This improved exposure correlated well with the Caco-2 permeability assay and predicted mouse microsomal clearance. Table 6 summarizes these data. Pyrazole **4c** with high Caco-2 permeability and medium predicted microsomal clearance had good exposure in mouse after oral dosing. In contrast, chloro indazole **21** with low Caco-2 permeability and high predicted mouse microsomal clearance had no detectable levels after oral dosing at any time points. Chloro indazole **23** possessed optimal ADME characteristics with high predicted Caco-2 permeability and low predicted microsomal clearance and demonstrated correspondingly good oral exposure in mice.

In summary, several replacements for an indanone–oxime were examined as inhibitors of B-Raf^{V600E} kinase. Naphthol and phenol were the most active replacements. Unfortunately, these head-groups led to poor rodent pharmacokinetics. Alternative head-groups also achieved good activity while certain examples demonstrated good pharmacokinetic exposure in rodents. Specifically, a tricyclic pyrazole and indazole demonstrated good oral exposure in mice, while indazoles could also be optimized for good cellular activity.

Acknowledgment

The authors thank Drs. Joachim Rudolph and Stefan Gradl for critical review of the manuscript and helpful suggestions.

References and notes

1. Peyssonnaux, C.; Eychene, A. *Biol. Cell* **2001**, *93*, 53.
2. Davies, H.; Bignell, G. R.; Cox, C.; Stephens, P., et al *Nature* **2002**, *417*, 949.

3. Pollock, P. M.; Harper, U. L.; Hansen, K. S.; Yudt, L. M., et al *Nat. Genet.* **2003**, *33*, 19.
4. (a) Gorden, A.; Osman, I.; Gai, W.; He, D.; Huang, W.; Davidson, A.; Houghton, A. N.; Busam, K.; Polsky, D. *Cancer Res.* **2003**, *63*, 3955; (b) Kuman, R.; Angelini, S.; Czene, K.; Sauroja, I.; Hahka-Kemppinen, M.; Pyrhonen, S.; Hemminki, K. *Clin. Cancer Res.* **2003**, *9*, 3362.
5. Wan, P. T.; Garnett, M. J.; Roe, S. M.; Lee, S.; Niculescu-Duvaz, D.; Good, V. M.; Jones, C. M.; Marshall, C. J.; Springer, C. J.; Barford, D.; Marais, R. *Cell* **2004**, *116*, 855.
6. (a) Samowitz, W. S.; Sweeney, C.; Herrick, J.; Albertsen, H.; Levin, T. R.; Murtaugh, M. A.; Wolff, R. K.; Slattery, M. L. *Cancer Res.* **2005**, *65*, 6063; (b) Riesco-Eizaguirre, G.; Gutiérrez-Martínez, P.; García-Cabezas, M. A.; Nistal, M.; Santisteban, P. *Endocr. Relat. Cancer* **2006**, *13*, 257; (c) Houben, R.; Becker, J. C.; Kappel, A.; Terheyden, P.; Bröcker, E. B.; Goetz, R.; Rapp, U. R. *J. Carcinog.* **2004**, *3*, 6.
7. Khazak, V.; Astsaturov, I.; Serebriiskii, I.; Golemis, E. *Expert Opin. Ther. Targets* **2007**, *11*, 1587.
8. Buckmelter, A. J.; Ren, L.; Laird, E. R.; Rast, B.; Miknis, G.; Wenglowsky, S.; Schlachter, S.; Welch, M.; Tarlton, E.; Grina, J.; Lyssikatos, J.; Brandhuber, B. J.; Morales, T.; Randolph, N.; Vigers, G.; Martinson, M.; Callejo, M. *Bioorg. Med. Chem. Lett.* **2010**. doi:10.1016/j.bmcl.2010.12.
9. Heberling, S.; Girreser, U.; Wolf, S.; Clement, B. *Biochem. Pharmacol.* **2006**, *71*, 354.
10. Inhibition of basal ERK phosphorylation in Malme-3M cells was used as the mechanistic cellular assay.
11. Hansen, J. D.; Grina, J.; Newhouse, B.; Welch, M.; Topalov, G.; Littman, N.; Callejo, M.; Gloor, S.; Martinson, M.; Laird, E.; Brandhuber, B. J.; Vigers, G.; Morales, T.; Woessner, R.; Randolph, N.; Lyssikatos, J.; Olivero, O. *Bioorg. Med. Chem. Lett.* **2008**, *28*, 4692.
12. Clement, B. *Drug Metab. Rev.* **2002**, *34*, 565.
13. Coordinates for B-Raf crystal structures have been deposited in the Protein Data Bank with accession codes 3PPJ (**1**), 3PPK (**12**), 3PRF (**19**) and 3PRI (**31**).
14. Uchaipichat, V.; MacKenzie, P.; Guo, X.; Gardner-Stephen, D.; Galetin, A.; Houston, J.; Miners, J. *Drug Metab. Dispos.* **2004**, *32*, 413.
15. Takle, A.; Brown, M.; Davies, S.; Dean, D.; Francis, G.; Gaiba, A.; Hird, A.; King, F.; Lovell, P.; Naylor, A.; Reith, A.; Steadman, J.; Wilson, D. *Bioorg. Med. Chem. Lett.* **2006**, *16*, 378.
16. Wilkening, R.; Ratcliffe, R.; Fried, A.; Meng, D.; Sun, W.; Colwell, L.; Lambert, S.; Greenlee, M.; Nilsson, S.; Thorsell, A.; Mojena, M.; Tudela, C.; Frisch, K.; Chan, W.; Birzin, E.; Rohrer, S.; Hammond, M. *Bioorg. Med. Chem. Lett.* **2006**, *16*, 3896.